IEEE Access
Multidisciplinary | Rapid Review | Open Access Journal

Received December 27, 2017, accepted January 22, 2018, date of publication January 29, 2018, date of current version March 13, 2018.

Digital Object Identifier 10.1109/ACCESS.2018.2799161

Fast Convergence Strategy for Multi-Image Superresolution via Adaptive Line Search

YINGQIAN WANG, (Student Member, IEEE), JUNGANG YANG, (Member, IEEE), CHAO XIAO, AND WEI AN

College of Electronic Science, National University of Defense Technology, Changsha 410073, China

Corresponding author: Jungang Yang (yangjungang@nudt.edu.cn)

ABSTRACT Multi-image superresolution (SR) techniques produce a high-resolution image from several low-resolution observations. Previous reconstruction-based SR approaches focus more on the optimization models but have not adequately emphasized the mathematic-solving techniques for this typically ill-conditioned and under-determined large scale problem. Since step size plays an important role in the iterative SR process, and there is a tradeoff between less computation cost and higher accuracy, conventional SR methods either adopt a fixed step size to obtain a higher running speed, or use a computationally expensive line search algorithm to pursue an improvement in accuracy. Taking both cues into consideration, in this paper, we propose an adaptive line search strategy to realize the fast convergence of reconstruction-based SR. The approximate analytical expression of step size is introduced to prevent us from setting it empirically or running iterations to test a proper one. We further modify the proposed strategy to be more adaptive under different SR conditions. Using our strategy, one can accelerate the SR process and obtain the optimal solution with less iteration. Experiments are conducted on both synthetic data sets and real-world scenes. The results have demonstrated the effectiveness and outperformance of our proposed strategy compared with other line search strategies.

INDEX TERMS Adaptive line search, approximate analytical expression, fast convergence, step size, superresolution.

I. INTRODUCTION

In many applications such as video surveillance [1]–[3], remote sensing [4]–[7] and medical diagnostics [8], [9], the demand for high-resolution (HR) images is continually increasing. However, it is usually impossible to achieve the desired resolution at the outset due to the technology and cost constrains [12]. As a result, digital image processing approach named *Superresolution* (SR) has been deeply studied to reconstruct an HR image from one or several degraded low-resolution (LR) observations. However, since much information is missed or suffers from noise in LR observations, SR reconstruction becomes an ill-posed problem, causing annoying blurs and artifacts in the restored HR image.

There are many researches on SR image reconstruction in the past three decades. Earlier research carried out by Tsai and Huang [10] was on frequency domain. As for spatial domain approaches, there are many famous algorithms such as non-uniform interpolation [11], [12], projection onto convex sets (POCS) [13], iterative back projection (IBP) [14] and Wiener filter based SR approach [30]–[32]. However, all of the approaches above have their own limitations and seem difficult to be further applied [12]. Recently, learning-based SR approaches [33]–[36] have drawn much attention due to the satisfactory reconstruction qualities. They learn the relations between LR and HR images from a given database. Note that the effectiveness of the learning-based algorithms highly depends on the training image database and this kind of algorithms generally requires a high computational complexity. In this paper, we focus on reconstruction-based methods [15]–[21] which formulate the SR process as an inverse problem with regularizations.

To obtain a satisfactory reconstruction result, *formulating a correct model*, *adopting a proper regularization term* and *employing an efficient mathematic solving algorithm* are three significant factors. The first two factors determine the optimal solution of the model whereas the last factor determines the computational complexity of reconstruction process and the quality of solution. For all reconstruction-based SR approaches, an image observation model is firstly

formulated. Then the observed LR images are utilized to estimate the original ideal HR image. The SR process is achieved by minimizing an objective function including two parts: 1) *fidelity term* to measure the error between the observed LR images and the simulated model outputs, 2) *regularization term* to apply priori knowledges to SR process.

Even though a correct model is formulated and a proper regularization term is adopted, the ideal reconstruction result cannot be easily acquired unless an efficient mathematic solving algorithm is employed to the problem. In [15], conventional steepest descend (SD) method with a fixed step size is used to find an optimal solution. The method is easily applied but performs a poor convergence. In [17], an SD method with a changing step size is adopted to accelerate the convergence. It generates results with a higher accuracy but cannot break the convergence limitation brought by the slow SD approach. Hardie *et al.* [22] employ a conjugate gradient (CG) method to solve SR problems and derive a changeable step size, which partly improves the convergence performance and shows its high computation speed. However, the design of step size lacks adaptiveness and robustness, performing less satisfyingly with various regularization terms and images. To further accelerate the convergence, Sorrentino and Antoniou [23], [24] utilize a powerful Quasi-Newton (QN) method to solve SR problems. The step size is calculated by an inexact line search method [25], which uses a series of iterations to test a suitable value. Although the method produces a satisfactory performance in accuracy and convergence, it requires a large amount of storage and computation, which is less suitable for further application.

In this paper, we propose an adaptive line search strategy to calculate a proper step size by deriving its approximate analytical expression, which can accelerate the convergence of SR reconstruction process and improve the accuracy of the solution. The algorithm is able to automatically adjust itself when dealing with different scenes and resolutions. It takes less time to generate a more accurate solution with less computation cost, which is suitable for promotion.

The rest of the paper is organized as follows: In *Section II*, we formulate the SR model and introduce the related work. In *Section III*, we outline our framework and introduce our proposed line search strategy with the corresponding adaptive modification. Experiments are conducted in *Section IV* with different line search strategies tested. Finally, we draw the conclusion in *Section V*.

II. FORMULATION OF SR MODEL

A. IMAGE DEGRADATION MODEL

As an inverse process of image degradation, SR reconstruction is tightly dependent on the image degradation model. Assume that a $\xi Q \times \xi Q$ HR image degrades into several $Q \times Q$ LR images, where $Q \times Q$ is the resolution of LR images and ξ is the sampling factor. We take various degrading factors into consideration and formulate the model as

$$Y_k = D_k H_k F_k X + N_k, \quad k = 1, 2, \ldots, N, \tag{1}$$

where $\xi^2 Q^2 \times 1$ vector X represents the original ideal HR image, the $Q^2 \times 1$ vector Y_k and N_k represent the k^{th} LR observed image and the additional Gaussian noise, respectively. X, Y_k and N_k are ordered lexicographically. The $Q^2 \times \xi^2 Q^2$ matrix D_k, the $\xi^2 Q^2 \times \xi^2 Q^2$ matrix H_k and F_k represent the down-sampling, blurring and warping process, respectively. Generally assuming that all LR images are generated under same conditions, we can further simplify the model into

$$Y_k = DHF_k X + N_k = W_k X + N_k, \quad k = 1, 2, \ldots, N, \tag{2}$$

where D and H respectively represent the down-sampling matrix and the blurring matrix, and they are same in all LR images. W_k is the total decimation matrix sized $Q^2 \times \xi^2 Q^2$, which has taken all the degrading factors above into consideration.

B. FIDELITY AND REGULARIZATION

The aim of SR reconstruction is to restore an HR image from the warped, blurred, down-sampled noisy LR images. In reconstruction-based SR framework, a cost function is always utilized to measure the distance between the estimations and the observations as

$$\hat{X} = \arg\min_X \left\{ \sum_{k=1}^{N} \| Y_k - W_k X \|_p^p \right\}, \quad k = 1, 2, \ldots, N. \tag{3}$$

It can be easily understood that a high-quality reconstructed image has to fit the LR observations through the formulated degradation model. However, as insufficient information given in LR observations, reconstructing the original HR image is an ill-posed and underdetermined problem, leading to inevitable artifacts. To solve the problem, various regularization terms are widely applied to introduce prior knowledges as

$$\hat{X} = \arg\min_X \left\{ \sum_{k=1}^{N} \| Y_k - W_k X \|_p^p + \lambda J(X) \right\}. \tag{4}$$

We further rewrite (4) into

$$\hat{X} = \arg\min_X f(X) = \arg\min_X \left\{ E_p(X) + \lambda J(X) \right\}. \tag{5}$$

In (5), $E_p(X)$ is called *fidelity term* which is an $L_p (1 \le p \le 2)$ norm expression measuring the distance between estimations and observations. In most reconstruction-based SR frameworks, p is generally set to the boundary values 1, 2 or their combination. It is claimed that L_1 norm is more robust and less sensitive to outliers at the expense of a worse convergence performance and an increasing difficulty in solving the minimization problem [26]. $J(X)$ is the *regularization term* representing the priori information and controlling the smoothness of the output image. For instance, Tikhonov regularization [16], [17] employs Laplacian operator to realize the prior that each pixel in natural image should not differ much from its neighbors. It effectively suppresses noise at the expense of blurring the edges. Many other regularization terms have been studied such as total variation (TV) [27], bilateral total

variation (BTV) [15], Markov random field (MRF) [20] and sparse representation [28]. Finally, λ is a scalar balancing the weight between fidelity and smoothness, which depends on the regularization terms and is generally set empirically.

C. OPTIMIZING TECHNIQUES

After the formulation of the SR model in (5), we can see that estimating an HR image is equivalent to finding the solution to minimize the objective function $f(X)$. For this minimization problem, there have been lots of mathematical algorithms to obtain numerical solutions such as SD method, CG method, Newton method, trust region method and QN method. Since SR problems are extremely large-scaled, Newton method and trust region method, where the Hessian matrix have to be derived, cannot suit the case. Even for SD, CG and QN method, the multiplications between matrices and vectors are generally operated in image space using warping, blurring and down-sampling operation. No matter which algorithm is employed, the updating scheme can be written into the following form

$$\hat{X}_{n+1} = \hat{X}_n + \beta_n d_n. \tag{6}$$

There are two key factors in the updating process: the *descent direction* d_n and the *step size* β_n. SD method adopts the negative gradient direction $d_n = -\nabla f(X_n)$ as the decent direction. CG method determines the current descent direction as a combination of the former descent direction and the current negative gradient direction, as follows

$$\begin{aligned} d_n &= -\nabla f(X_n) + \gamma_n d_{n-1} \\ \gamma_n &= \frac{\nabla f(X_n)^T \left(\nabla f(X_n) - \nabla f(X_{n-1})\right)}{d_{n-1}^T \left(\nabla f(X_n) - \nabla f(X_{n-1})\right)}. \end{aligned} \tag{7}$$

The descent direction of QN method is determined by $d_n = -S_n \nabla f(X_n)$, where S_n is a matrix generating an efficient descent direction at the expense of an increasing computation cost. The calculation and simplification of S_n is detailed in [23], [24]. The method is complicated but can achieve an improvement in accuracy.

The other significant factor is setting a proper step size, since an oversized step size will lead the iteration to a divergence whereas an undersized step size will cause a slow convergence. A general but less efficient strategy is to try different values and test a proper one, taking both stability and less computation cost into account. However, the optimal step size varies in different scenes, which is hard to be preset properly. Consequently, SR approach with a fixed step size faces a problem of lacking adaptiveness, and cannot always deliver a satisfactory performance. Another widely-used strategy is named *Line Search*, which derives β_n by minimizing the objective function

$$\beta_n = \arg\min_{\beta} f(X_n + \beta d_n). \tag{8}$$

Because of the complicated SR model and irregular differential terms, the optimal step size β_n is hard to be analytical expressed. Therefore, a general idea is to employ inexact line search strategies such as Armijo-Goldstein method [25] and Wolfe-Powell method [29] to achieve the optimal value by iterations. Although an accurate step size can improve the convergence, the line search process is also a large-scaled minimization problem which cannot be easily solved. Consequently, inexact line search strategies face a tradeoff between accuracy and computation cost. In order to improve the convergence performance of SR process and suppress the computation cost simultaneously, we design an efficient line search strategy.

Since the line search strategies have to work under an existing SR framework, after taking accuracy and computation cost into consideration, we adopt CG algorithm to generate the descent direction. Moreover, it should be noticed that *SR approaches with any effective descent direction can be improved with a more accurate step size using our line search strategy.*

III. ADAPTIVE LINE SEARCH STRATEGY UNDER A CG-BASED SR FRAMEWORK

In this section, we will introduce the CG-based SR approach, and infer our proposed line search strategy with the corresponding adaptive modification. We adopt L_2 norm as the fidelity term where the step size can be approximately analytical expressed. We employ BTV [15] as the regularization term but *any derivable regularization term is suitable for our strategy*. From the discussion above, we rewrite (5) into

$$\begin{aligned} \hat{X} &= \arg\min_X f(X) = \arg\min_X \{E_2(X) + \lambda J(X)\} \\ E_2(X) &= \sum_{k=1}^{N} \|Y_k - W_k X\|_2^2 \\ J(X) &= \sum_{l=-P}^{P} \sum_{m=0}^{P} \alpha^{|m|+|l|} \left\| X - S_x^l S_y^m X \right\|_1, \quad (l+m \geq 0) \end{aligned} \tag{9}$$

In (9), matrices S_x^l and S_y^m shift X by l and m pixels in horizontal and vertical directions, respectively. While shifting, boundaries are handled by padding the outermost pixels. The scalar weight $\alpha (0 < \alpha < 1)$ is applied to give a spatially decaying effect to the summation of the regularization terms.

A. CG-BASED SR FRAMEWORK

We first take the derivative of $f(X)$ in (9) and infer its gradient $\nabla f(X)$ as

$$\begin{aligned} \nabla f(X) &= -2 \sum_{k=1}^{N} W_k^T (Y_k - W_k X) + \lambda J'(X), \\ J'(X) &= \sum_{l=-P}^{P} \sum_{m=0}^{P} \alpha^{|m|+|l|} \left(I - S_y^{-m} S_x^{-l}\right) \\ &\quad \times sign\left(X - S_x^l S_y^m X\right), \quad (l+m \geq 0). \end{aligned} \tag{10}$$

The algorithm begins with an initial input obtained by interpolating the first LR image. The iterative procedure of CG-based SR framework is demonstrated in ***Algorithm* 1**.

Algorithm 1 Procedure of the CG-Based SR Framework

Input: interpolated HR estimation $\hat{X}_0$, initial descent direction $d_0 = -\nabla f(\hat{X}_0)$, set $n = 0$
A1: ***If*** stopping criterion is met, go to ***output***; ***else Do***:
A2: Employ a line search strategy to obtain a solution $\hat{\beta}$ from the problem $\arg\min_\beta\{f(X_n + \beta d_n)\}$
A3: $\hat{X}_{n+1} = \hat{X}_n + \hat{\beta} d_n$
A4: Calculate d_{n+1} according to (7)
A5: Set $n = n + 1$, go to ***A1***
Output: $\hat{X} = X_n$

B. APPROXIMATE ANALYTICAL EXPRESSION OF STEP SIZE

In this subsection, we will derive the approximate analytical expression of step size. To solve the line search problem in (8), we first take the derivate and obtain $\partial f/\partial\beta$ as

$$\frac{\partial f}{\partial \beta} = \frac{\partial f}{\partial (X+\beta d)} \cdot \frac{\partial (X+\beta d)}{\partial \beta} = d^T \cdot \frac{\partial f}{\partial (X+\beta d)}. \quad (11)$$

According to (10), we know that

$$\frac{\partial f}{\partial (X+\beta d)} = -2\sum_{k=1}^{N} W_k^T \{Y_k - W_k (X+\beta d)\} + \lambda J'(X+\beta d). \quad (12)$$

Set $d^T \cdot \frac{\partial f}{\partial (X+\beta d)} = 0$, and β can be solved as

$$\beta = \frac{d^T \cdot \left[\sum_{k=1}^{N} W_k^T (Y_k - W_k X) - 0.5\lambda J'(X+\beta d)\right]}{d^T \cdot \sum_{k=1}^{N} W_k^T W_k d}. \quad (13)$$

Here comes a problem that β cannot be extracted completely, *i.e.*, it exists on both sides of (13). A general solution is to set β on the right side as the value of last iteration and 0.1 for initialization. It is argued in *Section III-C* that fidelity error is much larger to regularization error at the beginning of the iteration. Therefore, different initial values of β make little difference to the calculated step size.

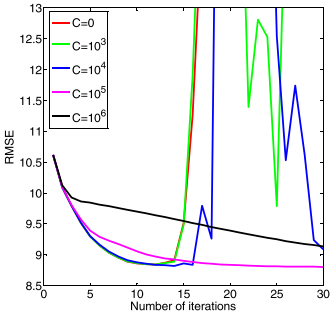

FIGURE 1. RMSE of SR reconstruction with ranged step size damping factor.

Unfortunately, due to the unideal quadratic property of the SR model, employing the step size in (13) directly cannot generate a stable solution. It leads to a divergence as the red curve shown in Fig. 1. To solve the problem, some schemes need to be adopted to stabilize and adapt the algorithm.

C. STABILITY AND ADAPTABILITY MODIFICATION

We analyze the stability of the proposed algorithm. Since CG-based SR method is inferred from a quadratic minimization problem, where it can show a best performance. But for non-quadratic problems with sharp changes in curvature function, there might be some problems with the method.

We begin our analysis from the change of fidelity term and regularization term with iterations. Consider that the initial input is generated by interpolation, which is with low sharpness and far from the final optimal solution. The L_2 norm fidelity error is much larger to the regularization error in early iterations, making the objective function more quadratic. However, as the iteration goes on, fidelity error has been constantly corrected and the reconstructed image becomes increasingly sharper. Then the regularization term shares a heavier weight, making the objective function increasingly non-quadratic. Since the BTV regularization term is a sum of L_1 norm errors, whose gradients change sharply at some points. The quadratic model based line search strategy always leads to a divergence with an oversized step size. Consequently, equation (13) has to be modified to stabilize the algorithm. Intuitionally, we add a scalar to the denominator in (13) as

$$\beta = \frac{d^T \cdot \left[\sum_{k=1}^{N} W_k^T (Y_k - W_k X) - 0.5\lambda J'(X+\beta d)\right]}{d^T \cdot \sum_{k=1}^{N} W_k^T W_k d + C}. \quad (14)$$

C can be understood as a damping factor to prevent β from becoming oversized. We calculate the step size according to (14) and combine it with CG-based SR algorithm. We adopt image *Butterfly* from *Set5 & Set14* Dataset as an example, reconstruct image with ranged values of C and use RMSE (20) to evaluate the quality of the reconstructed HR image. The convergence performance is depicted in Fig. 1.

We can learn from Fig. 1 that a smaller C can accelerate the convergence in earlier stage of iterations but cannot stabilize the solution in later period. In contrast, a larger C keeps the final solution stable but converges slowly. In order to realize the fast convergence property and obtain a final stable solution, C needs to change with iterations going on.

We first introduce a parameter η to express divergence degree, which is related to the L_2 norm of descent direction.

Algorithm 2 Procedure of the Proposed Adaptive Line Search Strategy

Input: β_{n-1}, η_{n-1}, $\hat{X}_n$, d_n, Y_k, W_k
A1: Calculate η_n according to (15)
A2: Calculate β_n according to (18)
Output: β_n, η_n, which will be used as an input in next iteration

The expression of η in the n^{th} iteration is shown as

$$\eta_n = \frac{\|d_n\|_2}{\sqrt{R_{ow}C_{ol}}}, \tag{15}$$

where d_n represents the descent direction of the estimated image in the n^{th} iteration, R_{ow} and C_{ol} represent row size and column size of HR image, respectively. Since the initial input has a distance to the optimal solution, d_n has a large norm at the beginning of iterations, which results to a large η. As iteration goes on, the error is corrected continuously and η reduces constantly. Conversely, it will lead to a divergence if η becomes lager with iterations. Inspired by the rule, we can judge the convergence condition by comparing divergence degrees of two neighboring iterations, which leads to our adaptability modification. To transform the divergence degree into a proper damping factor, we introduce *sigmoid function* as

$$y = \frac{1}{1 + \exp\{a\,(x - b)\}}, \quad (-\infty < x < +\infty), \tag{16}$$

where a is a decaying factor controlling the sensitivity and b is a shift factor controlling the threshold. The curve of sigmoid function is depicted in Fig. 2.

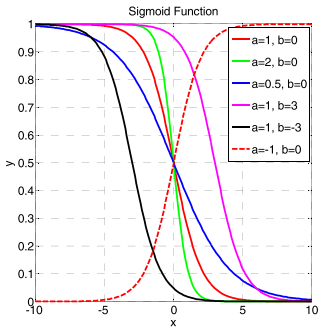

FIGURE 2. Sketch of sigmoid functions with ranged parameters.

We set parameters $a = 1$ and $b = 0$ in our implementation, and we transform the divergence degree into a damping factor as

$$C_n = \frac{R_{ow}C_{ol}}{1 + \exp\{\eta_n - \eta_{n-1}\}}. \tag{17}$$

We substitute (17) into (14) and get our proposed expression of step size as

$$\beta_n = \frac{d_n^T \cdot \left[\sum_{k=1}^{N} W_k^T \left(Y_k - W_k\hat{X}_n\right) - 0.5\lambda J'(\hat{X}_n + \beta_{n-1}d_n)\right]}{d_n^T \cdot \sum_{k=1}^{N} W_k^T W_k d_n + R_{ow}C_{ol}\left[1 + \exp\left(\eta_n - \eta_{n-1}\right)\right]^{-1}}. \tag{18}$$

The overall procedure of the proposed line search strategy is described in ***Algorithm 2***.

IV. EXPERIMENTS AND RESULTS

A. IMPLEMENTATION DETAILS

In this subsection, we introduce our implementation details methodically, including datasets and scenarios, compared methods, parameters setting and quantitative evaluation metrics. All experiments are coded in *MATLAB 2014a* and running on a *Core i7-5500U @ 2.40 GHz CPU* with a *12 GB RAM*.

• Dataset and scenarios

We conduct our experiment on two public datasets and real-world scenes, the public datasets are detailed as follows.

➢*Set5 & Set14 Dataset*

The dataset consists of 18 images with various resolutions. We use all of the images in the dataset in our experiment. The scene *Baboon* is selected to be analyzed and presented visually.

➢*BSD500 Dataset*

The dataset consists of 500 images (100 images in file *Test*, 200 images in file *Training* and 200 images in file *Value*) with the same resolution 481×321 or 321×481. We adopt 100 images from the file *Test* to run our algorithm and the scene *Children* is selected to be analyzed and presented visually.

➢*Real-world Scenes*

We employ our self-developed scanning gantry with a camera to capture the scene in our own laboratory. The devices are shown in Fig. 3. Similar to the flatbed scanner design proposed in [37], we shift the camera to the corners of a 1×1 cm^2 square and scan the scene. Due to the parallax in each captured sub-image, we can obtain 4 images of resolution 1424×1024 with subpixel shifts. After the operation of camera calibration [38], the sub-images can be applied to test the practicality of our strategy when dealing with real SR problems.

• Compared methods

In order to clearly demonstrate the superiority of our proposed line search strategy, we unify the descent directions into conjugate gradient direction and employ the following line search strategy as compared methods under both BTV and Tikhonov regularizations.

- ➢ Fixed step size [15]
- ➢ Lee's line search strategy [17]
- ➢ Hardie's line search strategy [22]
- ➢ Armijo line search strategy [23]

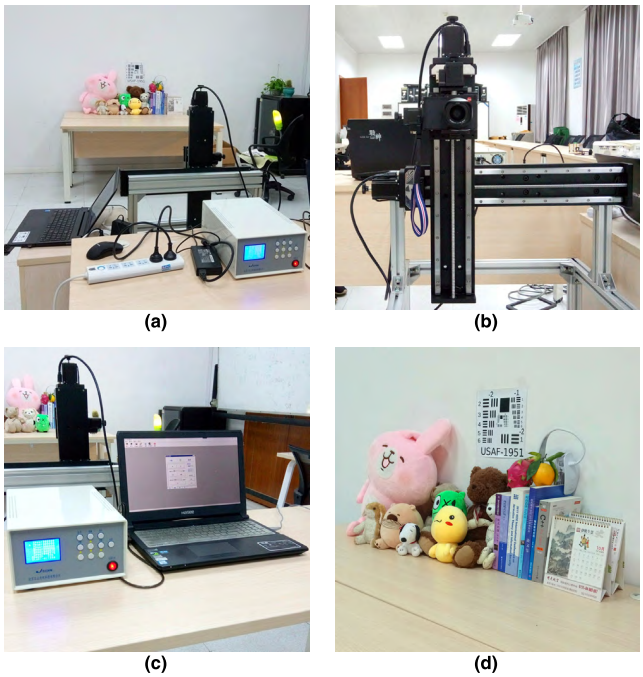

FIGURE 3. Self-developed SR imaging devices. (a) Overview of the real-world scene. (b) Scanning gantry with a camera. (c) Controller of the scanning gantry. (d) Objects which we use in experiments.

• Parameters

For synthetic scenes, LR images are generated and further adopted to reconstruct the HR image. In the degrading process, HR images are first warped by no more than 4 pixels to simulate the motion effect. Then the warped images are blurred by a 3×3 Gaussian kernel with $\sigma = 1$, which represents the optical blurring. Afterwards, the blurred frames are down-sampled by a factor $\xi = 2$. Finally, Gaussian noise with $\sigma_N = 1$ is added.

We employ BTV and Tikhonov regularization terms to our proposed strategy respectively. For all BTV-based SR approaches, we set $\alpha = 0.7$, $P = 2$, which are same as the values in [15]. For all Tikhonov-based SR approaches, we set the same Laplacian operator mentioned in [22] as

$$Lap = \begin{bmatrix} 0 & -0.25 & 0 \\ -0.25 & 1 & -0.25 \\ 0 & -0.25 & 0 \end{bmatrix}. \tag{19}$$

The quality of SR reconstruction depends enormously on the regularization weight, and the performance of SD method is largely related to the step size. We set these parameters as follows, which are confirmed to generate satisfactory results.

- ➢ For fixed step size strategy, the step size is set to 0.1.
- ➢ For all BTV based SR approaches, the regularization weight is set to 0.1.
- ➢ For all Tikhonov based SR approaches, the regularization weight is set to 0.2.

• Evaluation metrics

To evaluate and compare the reconstruction performance quantitatively, root mean square error (RMSE), peak signal-to-noise ratio (PSNR) and mean structure similarity (SSIM) are employed as metrics, which are defined as

$$\begin{cases} RMSE = \sqrt{\dfrac{\sum_{i=1}^{M}\sum_{j=1}^{N}\left[Y(i,j)-X(i,j)\right]^2}{MN}} \\ PSNR = 10\lg\dfrac{255^2 MN}{\sum_{i=1}^{M}\sum_{j=1}^{N}\left[Y(i,j)-X(i,j)\right]^2} \\ SSIM = \dfrac{(2\mu_x\mu_y + c_1)(2\sigma_x\sigma_y + c_2)}{(\mu_x^2+\mu_y^2+c_1)(\sigma_x^2\sigma_y^2+c_2)}, \quad \begin{cases} c_1 = (k_1 L)^2 \\ c_2 = (k_2 L)^2, \end{cases} \end{cases} \tag{20}$$

where M and N are the image size of row and column respectively, μ_x, μ_y are mean values and σ_x, σ_y are standard variance of image X and Y, respectively. c_1, c_2 are two stabilizing constants representing the dynamics of a pixel value, k_1 and k_2 are constants set to 0.01 and 0.03, respectively.

B. QUALITY OF SR RECONSTRUCTION

In this subsection, we fix the number of iterations to 10, upsample the images by a factor $\xi = 2$ and compare the reconstruction results both visually and quantitatively.

• Visual Quality

The reconstruction results of *Baboon, Children* and *Real-world Scene* are shown in Fig. 4-6, respectively.

We can see that the initial inputs generated by bicubic interpolation method blur the edge and texture regions remarkably with a serious loss of details. Compared with bicubic interpolation, fixed step size strategy has obvious SR effects with more clear details reconstructed, but cannot eliminate the blur adequately. Moreover, Lee's strategy, Hardie's strategy and Armijo line search strategy generate much the same HR images of relatively higher qualities. Among all of the competitive methods, reconstructions of superior visual qualities can be obtained by our proposed line search strategy. The proposed strategy can restore more details with fewer distortions under both BTV and Tikhonov regularizations.

• Quantitative Quality Metrics

We analyze the accuracy of the reconstruction results quantitatively. Notice that, since different strategies cost different time to reach different levels of accuracy, it makes less sense to compare the running time directly. We will transform the various strategies into a benchmark and further make an analysis in *Section IV-C*.

From Table 1, we learn that all of the strategies outperform bicubic interpolation method under both regularizations. SR with a fixed step size only gets the worst metrics among these strategies, indicating that all of the line search strategies can improve the convergence performance and accuracy to varying degrees. Specifically, Lee *et al.* and Hardie *et al.* reach a similar precision among these scenes, about 0.4 improvements in PSNR on average.

Armijo line search strategy performs as same as Lee *et al.* and Hardie *et al.* under Tikhonov regularization, but performs superiorly under BTV regularization with further 0.3 improvements in PSNR. It is mentionable that Armijo line

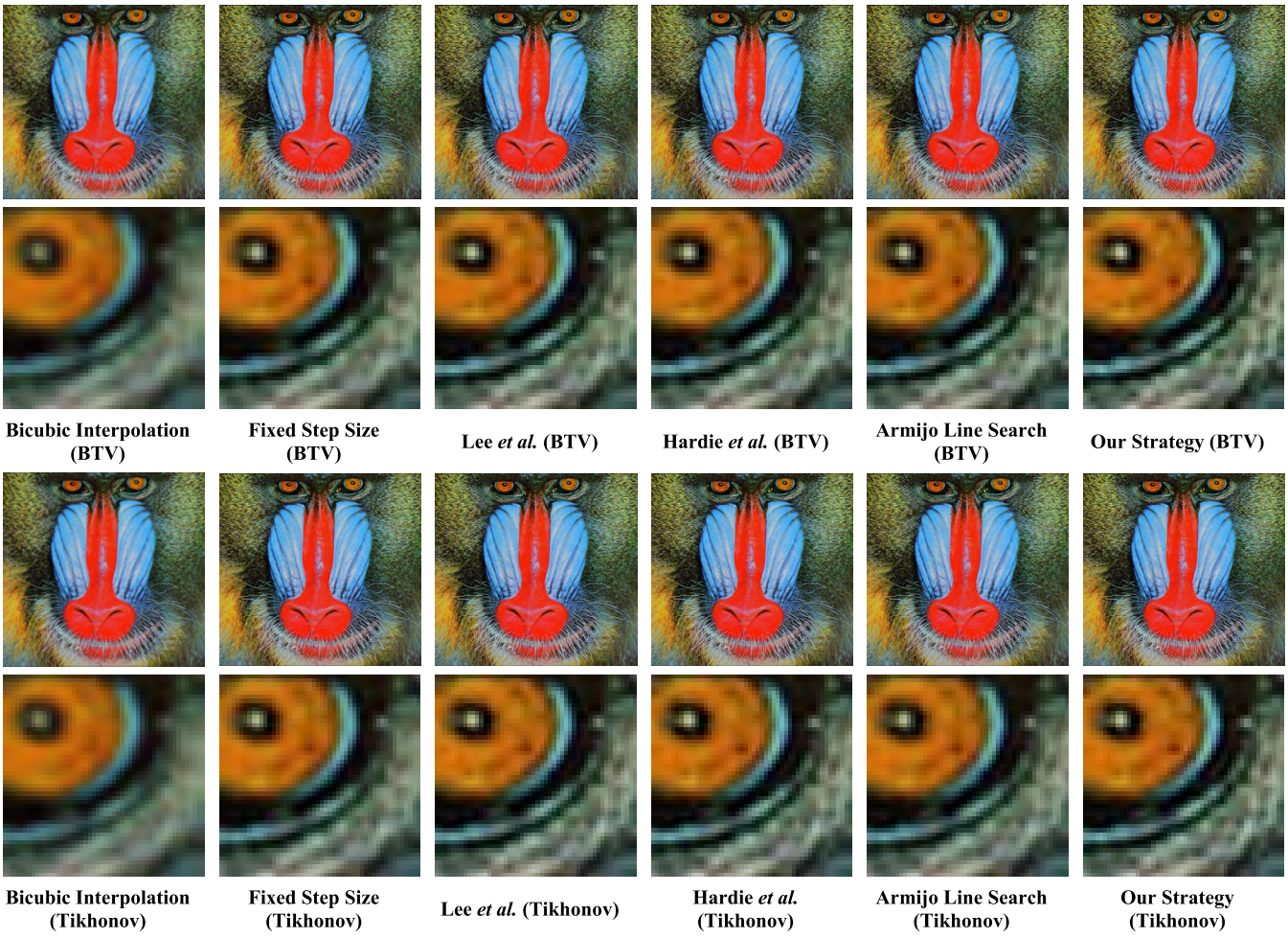

FIGURE 4. Visual comparison of image Baboon with BTV and Tikhonov regularizations. Sub-images in different columns correspond to different step size searching schemes.

TABLE 1. Quantitative result of accuracy.

BTV / Tikhonov	Line Search Strategy	Bicubic Interpolation	Fixed Step Size	Lee's Line Search	Hardie's Line Search	Armijo Line Search	Proposed
Baboon (500*480)	RMSE	20.97 / 20.97	18.31 / 18.35	17.74 / 17.54	17.81 / 17.68	17.30 / 17.79	17.03 / 17.22
	PSNR	20.64 / 20.64	21.81 / 21.79	22.08 / 22.18	22.05 / 22.11	22.30 / 22.06	22.44 / 22.34
	SSIM	0.824 / 0.823	0.902 / 0.903	0.913 / 0.918	0.912 / 0.915	0.922 / 0.913	0.926 / 0.924
Children (480*320)	RMSE	10.28 / 10.30	7.50 / 7.56	7.00 / 6.93	7.26 / 7.04	6.57 / 7.16	6.47 / 6.66
	PSNR	27.52 / 29.51	30.27 / 30.20	30.87 / 30.95	30.55 / 30.81	31.42 / 30.68	31.55 / 31.29
	SSIM	0.803 / 0.803	0.889 / 0.890	0.902 / 0.904	0.869 / 0.902	0.911 / 0.899	0.912 / 0.909
Average of *Set5 & Set14*	RMSE	11.74 / 11.74	9.21 / 9.29	8.79 / 8.84	8.82 / 8.80	8.52 / 8.78	8.33 / 8.63
	PSNR	26.81 / 26.81	28.99 / 28.91	29.40 / 29.34	29.36 / 29.37	29.64 / 29.39	29.84 / 29.53
	SSIM	0.875 / 0.875	0.919 / 0.918	0.924 / 0.922	0.924 / 0.922	0.926 / 0.923	0.929 / 0.926
Average of *BSD500*	RMSE	11.29 / 11.29	9.23 / 9.28	8.80 / 8.84	8.85 / 8.81	8.53 / 8.78	8.39 / 8.63
	PSNR	27.00 / 27.00	28.75 / 28.70	29.16 / 29.12	29.12 / 29.15	29.42 / 29.18	29.56 / 29.32
	SSIM	0.764 / 0.764	0.832 / 0.832	0.845 / 0.844	0.844 / 0.844	0.851 / 0.845	0.854 / 0.847

Note: Best results are colored in red and second best results are colored in blue.

search strategy gets a much satisfactory quantitative metrics in the scene *Children*, obtains over 0.5 increase in PSNR compared with Lee's and Hardie's strategies.

Among the compared strategies, our proposed line search strategy delivers best performances under both regularizations. When adopting our strategy under BTV

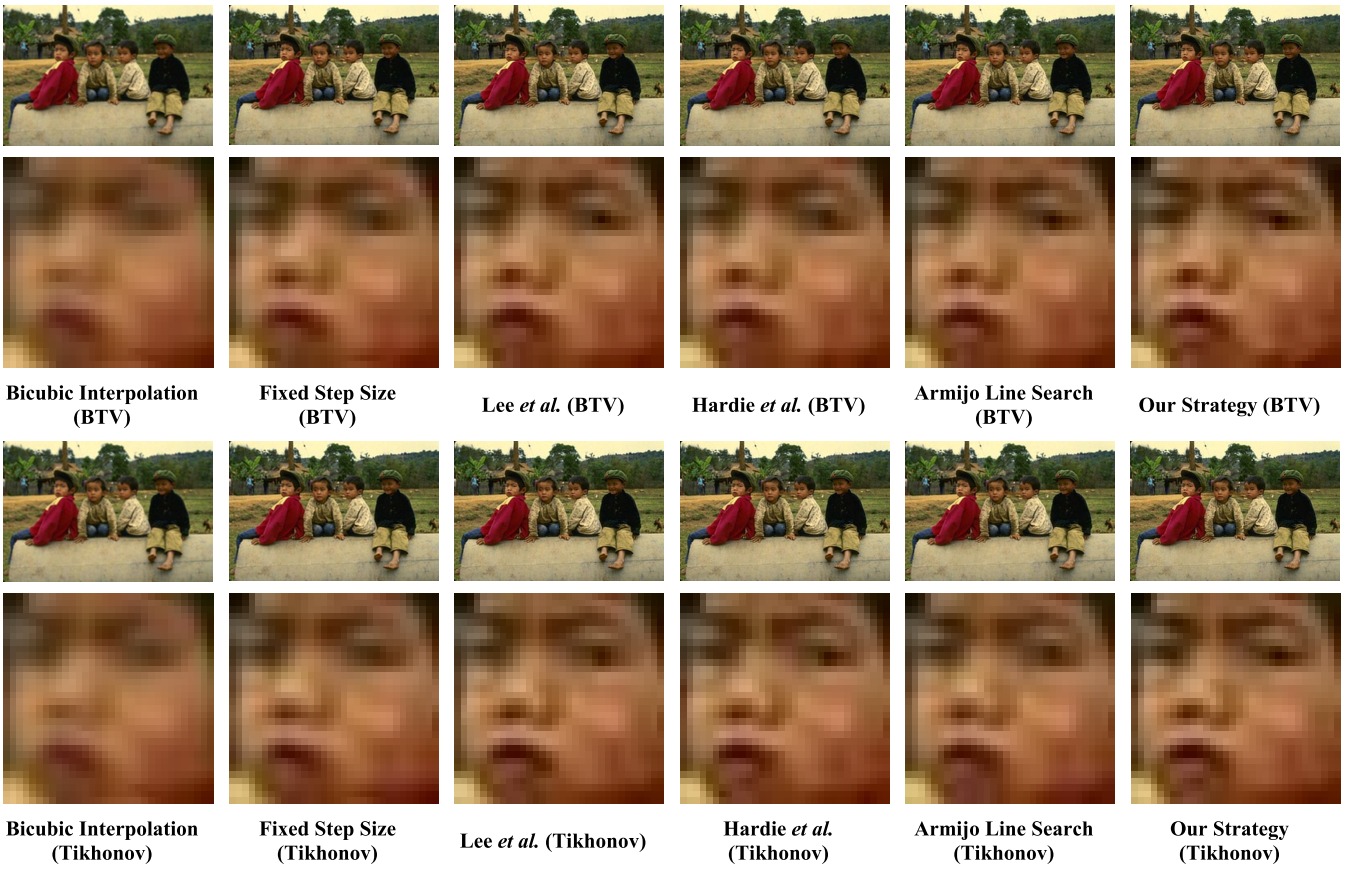

FIGURE 5. Visual comparison of image Children with BTV and Tikhonov regularizations. Sub-images in different columns correspond to different step size searching schemes.

regularization, further 0.15-0.2 improvements can be obtained compared with Armijo line search strategy. With regard to Tikhonov regularization, our proposed strategy can also generate at least 0.15-0.2 improvements over other strategies. The outperformance implies the commendable adaptability and robustness of our proposed line search strategy.

C. CONVERGENCE PERFORMANCE

In this subsection, we vary the number of iterations to study how the strategies converge to the solution. Afterwards, we investigate the efficiencies of strategies within a given running time. We use RMSE and PSNR to simply judge the qualities of reconstruction results.

• With ranged numbers of iterations

We firstly compare RMSE with 1-30 ranged numbers of iterations.

We can see from Fig. 7 that approaches perform differently under different regularizations. Our proposed strategy has a remarkable convergence performance with a superior decrease in RMSE under both regularizations. It generates a much more accurate solution with less iteration. Specifically, Armijo line search strategy performs a little worse than our strategy under BTV regularization but relatively worse under Tikhonov regularization. It means that Armijo line search strategy only fits the BTV regularization. Similarly, Hardie's strategy performs well under Tikhonov regularization but less satisfactorily with BTV regularization. In contrast, with both regularizations, our strategy not only converges fast but also generates solutions of the smallest RMSE under all iterations.

• With ranged running time

We notice that the fixed step size scheme has a worse convergence performance but a much faster running speed. In contrast, all of the line search strategies perform better in accuracy at the expense of an increasing time complexity. Since different strategies cost different time to reach different levels of accuracy, it is with great necessity to transform the strategies into a benchmark to compare their efficiencies, *i.e.*, to compare the SR quality within a given running time. The experimental results are shown in Fig. 8.

As running time increases, methods perform superiorly in different periods. In early period, the fixed step size scheme shows its advantages in fast computing and generates SR results of higher qualities. Afterwards, our proposed strategy performs better and generates solutions of a higher PSNR. Since results generated in early period have not converged to a stable optimal solution, the superiority of the fixed step size scheme in early period has less practical value but our proposed strategy shows its potential in SR application.

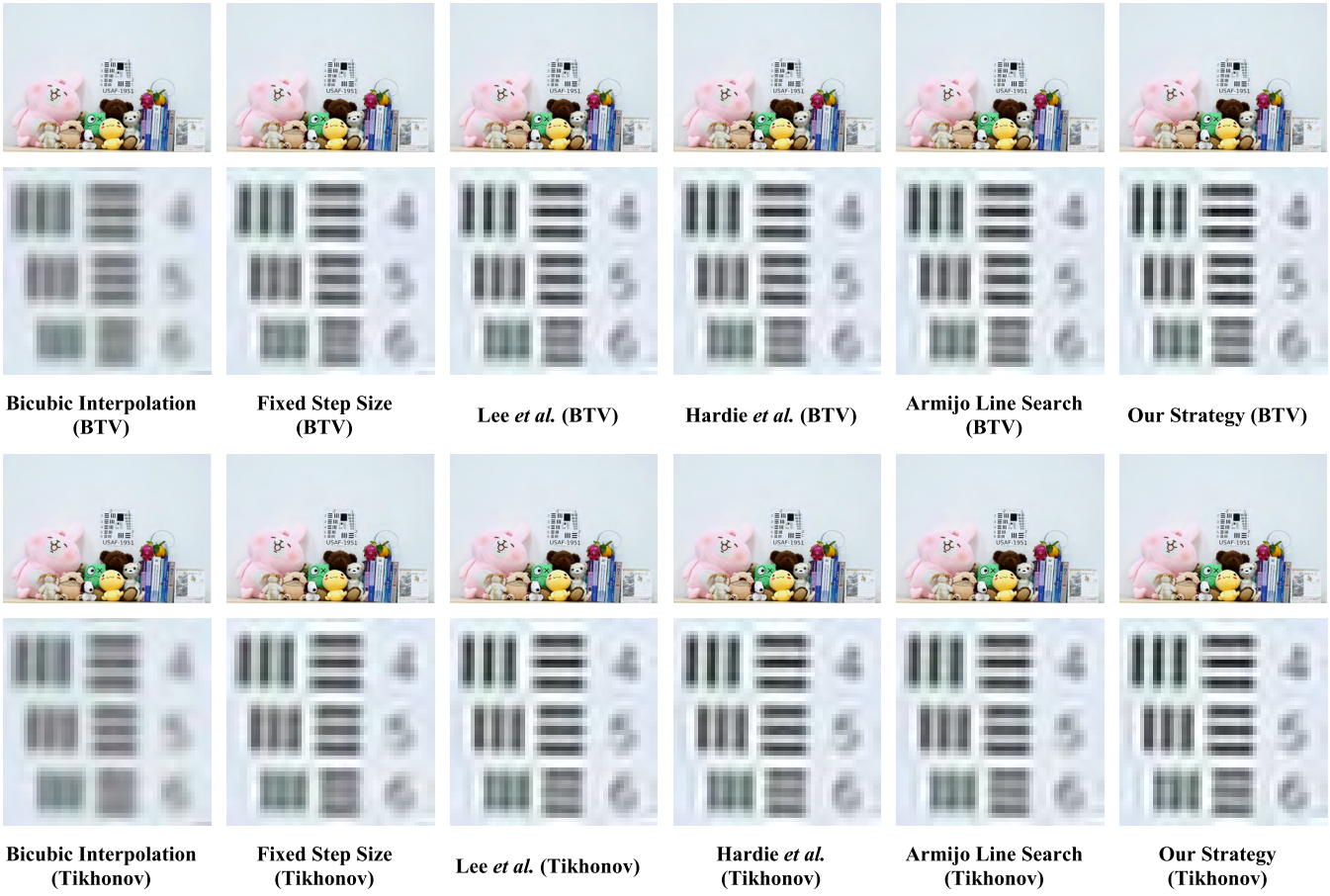

FIGURE 6. Visual comparison of Real-world Scene with BTV and Tikhonov regularizations. Sub-images in different columns correspond to different step size searching schemes.

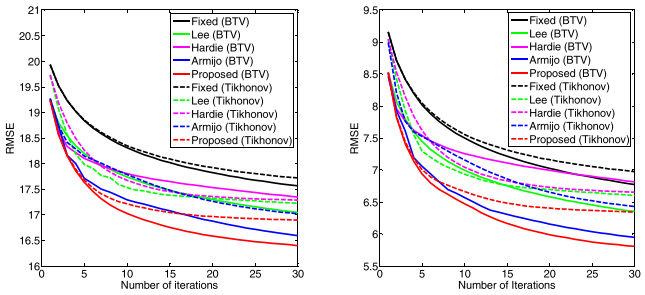

FIGURE 7. RMSE of scene Baboon and Children with ranged numbers of iterations. (a) Scene Baboon. (b) Scene Children.

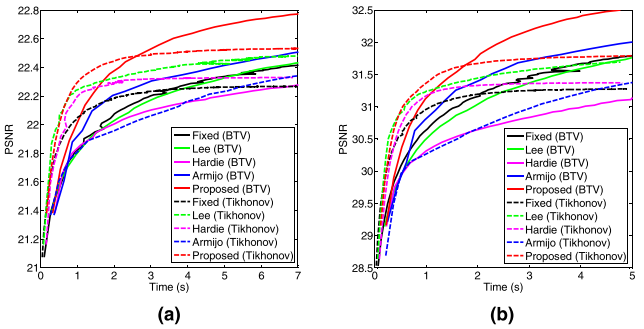

FIGURE 8. PSNR of scene Baboon and Children with ranged running time. (a) Scene Baboon. (b) Scene Children.

We can also noticed that although BTV-based SR approaches finally reach a higher precision than Tikhonov-based approaches, Tikhonov-based SR approaches perform better in early period since they cost less time per iteration. Consequently, if the SR situation requires a limited running time, Tikhonov-based SR approaches may suit the situation better.

Totally speaking, our proposed strategy with both BTV and Tikhonov regularization outperforms other strategies. It reaches a top SR quality on both quality-required and real-time-required SR occasions.

V. CONCLUSION

In this paper, we propose an adaptive line search strategy to calculate the step size in multi-image SR. Instead of using an empirical step size or test it by numerical iterative approach, we propose to infer its approximate analytical expression. We further improve its stability and adaptability by modifications, which avoid tuning parameters under various SR

conditions. Preliminary results show a remarkable improvement in the convergence and accuracy performance. Our line search strategy realizes a combination of high image quality and less computation cost, implying a great significance for further promotion.

REFERENCES

[1] V. Chandran, C. Fookes, F. Lin, and S. Sridharan, "Investigation into optical flow superresolution for surveillance applications," in *Proc. APRS Workshop Digit. Image Comput.*, 2005, vol. 26. no. 47, pp. 73–78.
[2] L. Zhang, H. Zhang, H. Shen, and P. Li, "A super-resolution reconstruction algorithm for surveillance images," *Signal Process.*, vol. 90, no. 3, pp. 848–859, 2010.
[3] T. Goto, T. Fukuoka, F. Nagashima, S. Hirano, and M. Sakurai, "Super-resolution system for 4K-HDTV," in *Proc. Int Conf. Pattern Recognit.*, Aug. 2014, pp. 4453–4458.
[4] A. J. Tatem, H. G. Lewis, P. M. Atkinson, and M. S. Nixon, "Super-resolution target identification from remotely sensed images using a Hopfield neural network," *IEEE Trans. Geosci. Remote Sens.*, vol. 39, no. 4, pp. 781–796, Apr. 2001.
[5] Y. Zhang, W. Li, Y. Huang, J. Yang, and Y. Zhang, "A fast iterative adaptive approach for scanning radar angular superresolution," *IEEE J. Sel. Topics Appl. Earth Observ. Remote Sens.*, vol. 8, no. 11, pp. 5336–5345, Nov. 2016.
[6] K. Makantasis, K. Karantzalos, A. Doulamis, and N. Doulamis, "Deep supervised learning for hyperspectral data classification through convolutional neural networks," in *Proc. IGARSS*, Jul. 2015, pp. 4959–4962.
[7] Y. Zhang, Y. Zhang, Y. Huang, J. Yang, and W. Li, "Super-resolution surface mapping for scanning radar: Inverse filtering based on the fast iterative adaptive approach," *IEEE Trans. Geosci. Remote Sens.*, vol. 56, no. 1, pp. 127–144, Jan. 2018.
[8] H. Greenspan, G. Oz, N. Kiryati, and S. Peled, "Super-resolution in MRI," in *Proc. ISBI*, 2002, pp. 943–946.
[9] W. Shi *et al.*, "Cardiac image super-resolution with global correspondence using multi-atlas patchmatch," in *Proc. Int. Conf. Med. Image Comput. Comput. Assist. Intervent.*, Jan. 2013, pp. 9–16.
[10] R. Y. Tsai and T. S. Huang, "Multiframe image restoration and registration," *Adv. Comput. Vis. Image Process.*, vol. 1, no. 2, pp. 317–339, 1984.
[11] N. Nguyen and P. Milanfar, "An efficient wavelet-based algorithm for image super resolution," in *Proc. Int. Conf. Image Process.*, Sep. 2000, pp. 351–354.
[12] S. Lertrattanapanich and N. K. Bose, "High resolution image formation from low resolution frames using Delaunay triangulation," *IEEE Trans. Image Process.*, vol. 11, no. 12, pp. 1427–1441, Dec. 2002.
[13] H. Stark and P. Oskoui, "High-resolution image recovery from image-plane arrays, using convex projections," *J. Opt. Soc. Amer. A, Opt. Image Sci.*, vol. 6, no. 11, pp. 1715–1726, 1989.
[14] M. Irani and S. Peleg, "Improving resolution by image registration," *CVGIP, Graph. Models Image Process.*, vol. 53, no. 3, pp. 231–239, May 1991.
[15] S. Farsiu, M. D. Robinson, M. Elad, and P. Milanfar, "Fast and robust multiframe super resolution," *IEEE Trans. Image Process.*, vol. 13, no. 10, pp. 1327–1344, Oct. 2004.
[16] X. Zhang, E. Y. Lam, E. Wu, and K. K. Y. Wong, "Application of Tikhonov regularization to super-resolution reconstruction of brain MRI images," in *Medical Imaging and Informatics* (Lecture Notes in Computer Science), vol. 4987. Berlin, Germany: Springer, 2008, pp. 51–56.
[17] E. S. Lee and M. G. Kang, "Regularized adaptive high-resolution image reconstruction considering inaccurate subpixel registration," *IEEE Trans. Image Process.*, vol. 12, no. 7, pp. 826–837, Jul. 2003.
[18] M. Elad and A. Feuer, "Restoration of a single superresolution image from several blurred, noisy, and undersampled measured images," *IEEE Trans. Image Process.*, vol. 6, no. 12, pp. 1646–1658, Dec. 1997.
[19] H. Shen, L. Zhang, B. Huang, and P. Li, "A MAP approach for joint motion estimation, segmentation, and super resolution," *IEEE Trans. Image Process.*, vol. 16, no. 2, pp. 479–490, Feb. 2007.
[20] R. Molina, J. Mateos, A. K. Katsaggelos, and M. Vega, "Bayesian multichannel image restoration using compound Gauss-Markov random fields," *IEEE Trans. Image Process.*, vol. 12, no. 12, pp. 1642–1654, Dec. 2003.
[21] F. Humblot and A. Mohammad-Djafari, "Super-resolution using hidden Markov model and Bayesian detection estimation framework," *EURASIP J. Appl. Signal Process.*, vol. 2006, no. 1, p. 36971, Dec. 2006.
[22] R. C. Hardie, K. J. Barnard, J. G. Bognar, E. E. Armstrong, and E. A. Watson, "High-resolution image reconstruction from a sequence of rotated and translated frames and its application to an infrared imaging system," *Opt. Eng.*, vol. 37, no. 1, pp. 247–260, 1998.
[23] D. A. Sorrentino and A. Antoniou, "Multiframe image superresolution using quasi-Newton algorithms," in *Proc. IEEE Int. Symp. Circuits Syst.*, May 2008, pp. 264–267.
[24] D. A. Sorrentino and A. Antoniou, "Improved hybrid demosaicing and color super-resolution implementation using quasi-Newton algorithms," in *Proc. Can. Conf. Elect. Comput. Eng.*, 2009, pp. 815–818.
[25] L. Grippo, F. Lampariello, and S. Lucidi, "A nonmonotone line search technique for Newton's method," *SIAM J. Numer. Anal.*, vol. 23, no. 4, pp. 707–716, 1986.
[26] Y.-R. Li, D.-Q. Dai, and L. Shen, "Multiframe super-resolution reconstruction using sparse directional regularization," *IEEE Trans. Circuits Syst. Video Technol.*, vol. 20, no. 7, pp. 945–956, Jul. 2010.
[27] L. I. Rudin, S. Osher, and E. Fatemi, "Nonlinear total variation based noise removal algorithms," *Phys. D, Nonlinear Phenomena*, vol. 60, nos. 1–4, pp. 259–268, 1992.
[28] J. Yang, J. Wright, T. S. Huang, and Y. Ma, "Image super-resolution via sparse representation," *IEEE Trans. Image Process.*, vol. 19, no. 11, pp. 2861–2873, Nov. 2010.
[29] V. Torczon, "On the convergence of pattern search algorithms," *SIAM J. Optim.*, vol. 7, no. 1, pp. 1–25, 1993.
[30] R. Hardie, "A fast image super-resolution algorithm using an adaptive Wiener filter," *IEEE Trans. Image Process.*, vol. 16, no. 12, pp. 2953–2964, Dec. 2007.
[31] B. N. Narayanan, R. C. Hardie, and E. J. Balster, "Multiframe adaptive Wiener filter super-resolution with JPEG2000-compressed images," *Eurasip J. Adv. Signal Process.*, vol. 2014, no. 1, p. 55, 2014.
[32] M. S. Alam, J. G. Bognar, R. C. Hardie, and B. J. Yasuda, "Infrared image registration and high-resolution reconstruction using multiple translationally shifted aliased video frames," *IEEE Trans. Instrum. Meas.*, vol. 49, no. 5, pp. 915–923, Oct. 2002.
[33] J. Kim, J. K. Lee, and K. M. Lee, "Accurate image super-resolution using very deep convolutional networks," in *Proc. IEEE Comput. Soc. Comput. Vis. Pattern Recognit.*, Jun. 2016, pp. 1646–1654.
[34] W. Shi *et al.*, "Real-time single image and video super-resolution using an efficient sub-pixel convolutional neural network," in *Proc. IEEE Conf. Comput. Vis. Pattern Recognit.*, Jun. 2016, pp. 1874–1883.
[35] X.-Y. Jing *et al.*, "Super-resolution person re-identification with semi-coupled low-rank discriminant dictionary learning," *IEEE Trans. Image Process.*, vol. 26, no. 3, pp. 1363–1378, Mar. 2017.
[36] K. Zhang, D. Tao, X. Gao, X. Li, and Z. Xiong, "Learning multiple linear mappings for efficient single image super-resolution," *IEEE Trans. Image Process.*, vol. 24, no. 3, pp. 846–861, Mar. 2015.
[37] J. C. Yang *et al.*, "A light field camera for image based rendering," Ph.D. dissertation, Dept. Elect. Eng. Comput. Sci., Massachusetts Inst. Technol., Cambridge, MA, USA, 2000.
[38] Z. Zhang, "A flexible new technique for camera calibration," *IEEE Trans. Pattern Anal. Mach. Intell.*, vol. 22, no. 11, pp. 1330–1334, Nov. 2000.

YINGQIAN WANG received the B.E. degree in electric engineering from Shandong University, Shandong, China, in 2016. He is currently pursuing the M.E. degree with the College of Electronic Science, National University of Defense Technology, Changsha, China. His research interests include light field imaging, superresolution, image fusion, and light field depth recovery. Mr. Wang has gained the China National Scholarship in 2013, 2014, and 2015, respectively, and received the first prize in the final of the 6th Chinese Mathematics Competitions in 2014.

JUNGANG YANG received the B.E. degree in electronic engineering, the M.E. degree, and the Ph.D. degree in information and communication engineering from the National University of Defense Technology (NUDT), Changsha, China, in 2007, 2008, and 2013 respectively. From 2011, he was a Visiting Ph.D. Student with The University of Edinburgh, Edinburgh, U.K. He is currently a Lecturer with the College of Electronic Science, NUDT. His research interests include computational imaging, image processing, compressive sensing, and sparse representation. Dr. Yang was a recipient of the New Scholar Award of Chinese Ministry of Education in 2012, the Youth Innovation Award and the Youth Outstanding Talent of NUDT in 2016. He was sponsored by the Innovation Project of the NUDT for Excellent Graduate Student in 2012.

CHAO XIAO received the B.E. degree in the communication engineering from the National University of Defense Technology, Changsha, China, in 2016, where he is currently pursuing the M.E. degree with the College of Electronic Science. His research interests include light field imaging and camera calibration.

WEI AN received the Ph.D. degree from the National University of Defense Technology (NUDT), Changsha, China, in 1999. She was a Senior Visiting Scholar with the University of Southampton, Southampton, U.K., in 2016. She is currently a Professor with the College of Electronic Science, NUDT. She has authored or co-authored over 100 journal and conference publications. Her current research interests include signal processing and image processing.